Production scraps to raw materials: low-cost method for implementing lithium iron phosphate cathode scraps back to production lines

Original
Production scraps to raw materials: low-cost method for implementing lithium iron phosphate cathode scraps back to production lines / Lassila, Lotta Liina; Bruno, Martina; Francia, Carlotta; Santasalo-Aarnio, Annukka; Gandolfo, Matteo; Fiore, Silvia. - In: JOURNAL OF POWER SOURCES. - ISSN 0378-7753. - 671:(2026), pp. 1-12. [10.1016/j.jpowsour.2026.239558]

Publisher:
Elsevier

Published
DOI:10.1016/j.jpowsour.2026.239558

Journal of Power Sources 671 (2026) 239558

Contents lists available at ScienceDirect

Journal of Power Sources

journal homepage: www.elsevier.com/locate/jpowsour

Production scraps to raw materials: low-cost method for implementing lithium iron phosphate cathode scraps back to production lines

Lotta Liina Lassila [a,b,c], Martina Bruno [a], Carlotta Francia [b], Annukka Santasalo-Aarnio [c], Matteo Gandolfo [b], Silvia Fiore [a,*]

[a] DIATI, Department of Environment, Land, and Infrastructure Engineering, Politecnico di Torino, Corso Duca degli Abruzzi 24, 10129, Turin, Italy
[b] DISAT, Department of Applied Science and Technology, Politecnico di Torino, Corso Duca degli Abruzzi 24, 10129, Turin, Italy
[c] Aalto University, Department of Energy and Mechanical Engineering, Research Group of Energy Conversion and Systems, Otakaari 4, 00076, Espoo, Finland

HIGHLIGHTS

- Low-temperature direct recycling aids LFP production scraps closed-loop recycling.
- 400 °C N_2 treatment allows 100% recycling of LFP scraps with good performance.
- 30% of 200 °C air recycled LFP is blended in new slurry without performance loss.
- Recycling reduces slurry material costs and CO_2 footprint below virgin material.

GRAPHICAL ABSTRACT

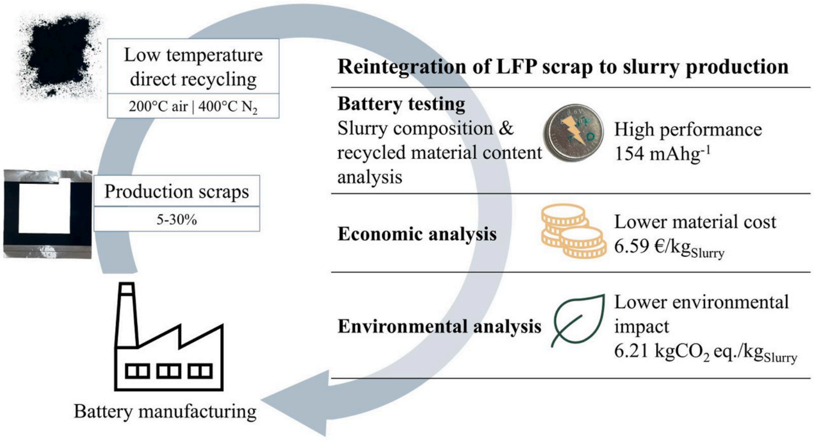

ARTICLE INFO

Keywords:
Battery
Circular economy
Direct recycling
LFP
Production scraps

ABSTRACT

In recent years, the increased production of lithium-ion batteries (LIBs) has been causing significant amounts of production scraps that require efficient, economical, and environmentally viable recycling methods. This study investigates strategies for integrating low-temperature direct recycling of lithium iron phosphate (LFP) production scraps into battery manufacturing. Scrap LFP cathode active material (CAM) was direct recycled at 200 °C in air and 400 °C in N_2. The recycled CAM was blended in different amounts (100, 50, 30%-wt) with commercial CAM. Two slurry compositions were considered based on CAM: polyvinylidene fluoride: carbon black ratios (80:10:10 and 92:5:3), and coin cells were manufactured and tested. Results indicate that recycled CAM can be directly reprocessed in new batteries exhibiting excellent electrochemical performance (154 mAh g^{-1}, equivalent to pristine material) when the slurry included 30%-wt CAM recycled at 200 °C in air and 100%-wt CAM recycled at 400 °C in N_2. Compared to virgin slurry material cost (9.06 €/kg_{slurry}) and environmental impact (8.27 kg CO_2/kg_{slurry}), incorporating 30%-wt CAM recycled at 200 °C in air reduced costs to 6.59

---

[*] Corresponding author.
E-mail address: silvia.fiore@polito.it (S. Fiore).

https://doi.org/10.1016/j.jpowsour.2026.239558
Received 5 November 2025; Received in revised form 1 February 2026; Accepted 3 February 2026

€/kg_{Slurry} and emissions to 6.21 $kgCO_2/kg_{slurry}$, and 100%-wt CAM recycled at 400 °C in N_2 corresponded to 3.77 €/kg_{Slurry} and 2.45 $kgCO_2/kg_{slurry}$. These findings clearly demonstrate that closed-loop integration of low-temperature direct recycling of LFP cathode scraps into cell manufacturing reduces material costs and environmental impact while maintaining high electrochemical performance.

1. Introduction

The rapid expansion of global battery manufacturing has led to numerous new production lines [1]. Up to 30%-wt of the final products from these production lines can be classified as production scraps originating from quality checks, trimmings etc. [2]. Scrap production typically decreases to 5-10%-wt as operations stabilise [3]. Since production scrap is generated constantly in manufacturing, it presents an immediate material source for battery recycling, in contrast to End-of-Life (EoL) batteries, which only become available after years of service [1]. Recycling production scraps fundamentally differs from recycling EoL batteries, mainly because scrap materials have not been exposed to electrolyte and degradation from electrochemical cycling [4]. State-of-the-art destructive and resource-intense battery recycling methods involving pyro- and hydrometallurgy, specifically designed for cobalt-rich cathode active material (CAM) [5], are generally excessive for pristine production scraps [6]. These methods are also unprofitable for recycling lithium iron phosphate (LFP) CAM due to the low cost of virgin active material [7,8]. This creates a knowledge gap between the available recycling technologies and the practical needs of LFP production scrap management. Policy and market developments are raising the urgency of closing this gap. Batteries are a vital part of the green transition, and legislative frameworks are increasingly designed to enhance sustainability while strengthening supply chain resilience and reducing dependency on third-party material sources. The European Union (EU) has introduced comprehensive battery regulations including recycling targets, minimum recycled content thresholds, and mandatory carbon footprint reporting as well as restricted battery waste exports [9,10]. These legislative developments not only create pressure but also open opportunities for manufacturers to adopt solutions that reintegrate secondary battery materials into production lines. Recycling of production scrap therefore emerges as a particularly promising strategy to align industrial practice with upcoming regulatory requirements.

In response to these challenges and regulatory drivers, one of the most promising strategies for production scrap recycling is direct recycling, a non-destructive alternative to conventional recycling methods where the active material is recovered and directly reintegrated into battery production [5]. Especially with pristine production scraps, only limited regeneration is needed [6], and the main challenge is the detachment of CAM from the current collector through the degradation of polyvinylidene fluoride (PVDF) binder [11]. High stability of PVDF makes the detachment technically challenging, and chemical and thermal recycling methods are commonly applied [11]. Chemical methods involve dissolving the binder in a solvent such as N-methyl-2-pyrrolidone, which is highly toxic [4] or in green solvents such as cyrene [12], propylene carbonate [13] and ethylene glycol [14]. Nevertheless, green solvents are expensive [15], can alter the active material surface chemistry [16], and require multiple post-treatment steps hindering industrial scale-up. Thermal treatment at around 600 °C fully removes PVDF [17,18], but it is energy-intensive and makes the recycling process more sensitive to energy market fluctuations. High temperature can also cause LFP oxidation and pose safety and environmental concerns due to the release of hazardous hydrogen fluoride (HF) from PVDF decomposition [15,19,20].

Low-temperature LIB recycling methods have been previously studied as cost-effective and environmentally friendly alternatives [4,18,21–26]. However, previous research has mainly addressed EoL batteries [23,25–27], and CAM chemistries rich in cobalt and nickel [4,18,22,24,28,29] with just few studies considering LFP production scraps [21]. The key knowledge gaps in the topic are the absence of reintegration of direct-recycled LFP production scraps back to cell production, and the lack of studies assessing the related economic and environmental aspects.

This study aims to fill these knowledge gaps, and it builds on the research presented in a previous study [30], which concluded that low temperature direct recycling of production scrap CAM provides significant economic and environmental benefits. In the mentioned study, production scrap CAM samples including LFP and Lithium nickel manganese cobalt oxides (NMC) were heated for 30 min in either air or nitrogen across a temperature range between 200 and 600 °C. The results demonstrate that LFP CAM direct recycling at 200 °C in air yielded the lowest cost (0.71 €/kg) and environmental impact (1.18 kg CO_2eq) compared to all other tested conditions, though residual PVDF remained in the recovered material. In contrast, LFP CAM recycling in nitrogen at 400 °C improved PVDF removal while preventing LFP oxidation and maintaining lower costs (2.36 €/kg) and emissions (2.02 kg CO_2eq) compared to conventionally applied 600 °C. Specifically, the previous study mentioned focused on the direct recycling process optimization for LFP and NMC cathode production scraps and on the related economic and environmental aspects. On the other hand, the present study has as its main objective and novelty to investigate the practical implementation of an on-site, low-temperature direct recycling process applied exclusively to LFP cathode production scraps, with a specific focus on reintegrating the recovered CAM into the manufacturing of new cells. This is particularly relevant as the EU Battery Regulation requires manufacturers to include a share of recycled material in new batteries starting from 2031 [10]. The direct recycling method presented here could help meet these targets, but it is essential that cells containing recycled material maintain high electrochemical performance and that the economic and environmental impact is thoroughly studied.

The key research question of the present study is to identify how much recycled LFP CAM can be included in the slurry for the manufacturing of new cells without compromising the electrochemical performance, in comparison with pristine CAM. In this study, LFP cathode scraps that underwent direct recycling at 200 °C in air and at 400 °C in nitrogen were characterized and incorporated in two slurry formulations, identified as reference composition for CAM testing and typical industrial composition. Reference slurry formulations included definition of different shares of recycled LFP (100, 50 and 30%-wt) blended with commercial CAM to define the maximum viable concentration yielding good electrochemical performance, which was then applied to the industrially relevant slurry composition. Finally, a critical assessment of the economic and environmental viability of the proposed short-loop recycling strategy is proposed.

2. Materials and methods

The experimental workflow (Fig. 1) involved direct recycling of LFP scrap CAM samples, recycled material characterisation, production of slurry and coin cells, and electrochemical testing of the cells. Direct recycling of LFP cathode production scraps involved three phases: a thermal treatment, ball milling and sieving. The process conditions leading to best economic and environmental performances in the mentioned previous study [30] were selected, e.g. thermal treatment at 200 °C in air and at 400 °C in N_2.

The main goal of this study is to identify how much recycled CAM can be included in a new cell and the corresponding electrochemical performances. Standard coin cells were manufactured via solvent tape casting method adopting two slurry compositions: (i) a mixture of 80%-wt active material, 10%-wt PVDF and 10%-wt carbon black (referred to as 80:10:10 in the following) that is typical for testing the electrochemical performance of CAM; and (ii) an industry-relevant mixture with 92%-wt active material, 5%-wt PVDF and 3%-wt carbon black (referred to as 92:5:3 in the following) [31]. The active material included in the two slurry compositions encompassed different shares of recycled LFP CAM (100, 50, 30 and 0%) and commercial CAM (0, 50, 70 and 100%). The selected recycled CAM proportions were chosen to assess whether the maximum potential industrial scrap generation (>30%) [3]) can be reintegrated into slurry production via direct recycling, without compromising electrochemical performance or economic and environmental feasibility.

2.1. Materials and equipment for direct recycling

LFP production scraps with composition of 92 %-wt CAM, 5 %-wt PVDF and 3%-wt carbon black were supplied by the National Research and Development Institute for Cryogenic and Isotopic Technologies – ICSI Rm. Valcea, Romania. Direct recycling of LFP cathode production scraps happened in a GERO TF1 Carbolite tubular muffle furnace at 200 °C in air (this condition is identified as 200 °C air in the following) and at 400 °C in nitrogen (2 L/min flow) (this condition is identified as 400 °C N_2 in the following). 2 g of scrap CAM was inserted in the furnace at room temperature, heated at 5 °C/min, held in the target temperature for 30 min and cooled down at 4 °C/min. Thermal treatment was followed by milling for 5 min in a MM200 Retsch ball mill with zirconium oxide jars and beads. After ball milling, the active material was separated from aluminium current collectors by sieving at 0.1 mm. The direct recycling process was repeated multiple times to obtain enough recycled LFP CAM for the subsequent characterisation and slurry production steps for each process condition.

This study considered commercial pulverized LFP of M12 series from ALEEES as reference commercial material.

2.2. Characterization of cathodic active materials

Thermogravimetric analysis (TGA) (NETZSCH TG 209 F3 and TA Instruments TGA 5500) was performed under N_2 atmosphere at a heating rate of 10 °C min^{-1} from 30 up to 600 °C to quantify the PVDF residual content in the scrap and recycled CAM samples. Fourier-transform infrared (FTIR) spectrometry (Thermo Fisher Nicolet Summit) was employed to confirm the presence of PVDF. The crystal structure and phase composition of the materials was determined by X-ray diffraction (XRD) spectroscopy (PANalytical X'Pert) with a Cu Kα radiation and a 2θ scan range from 10° to 70°, while the microstructure, morphology and element distribution were examined using field emission scanning electron microscopy (FESEM)(Zeiss, SUPRA 40) and Scanning electron microscopy with energy-dispersive X-ray spectroscopy (SEM-EDX) (Zeiss, Sigma VP) The Al impurity content in recycled cathode material was analysed with Flame atomic absorption spectroscopy (FAAS) (Schimadzu, GFA-EX7). The cathode active materials' surface composition was determined with X-ray photoelectron spectroscopy (XPS)(Kratos, Axis Ultra ESCA).

2.3. Production of coin cells

The electrodes constituting the coin cells were prepared by solvent tape casting method [32] employing TIMCAL C-NERGYTM Super C65 carbon black and HSV900 PVDF solution in N-methyl pyrrolidone (NMP) (Sigma-Aldrich) with variable contents of recycled and commercial LFP CAM and considering the two slurry compositions mentioned (80:10:10 and 92:5:3). The recycled CAM content was initially set at 100% to evaluate its standalone electrochemical performance. Subsequently, the recycled content was reduced (50% and 30%-wt blended with commercial CAM) to determine the maximum recycled material content for both recycled CAM materials that provides electrochemical performance comparable to pristine commercial LFP.

The slurries were homogenized using a Retsch MM200 ball mill for 15 min at 30 Hz and then casted onto aluminium foil (ARMOR Group, 19.8 μm thick) using a Sheen 113N automatic film applicator at a speed of 50 mm s^{-1} and adjusted to 200 μm thickness. After solvent evaporation at 50 °C for 1 h, electrode disks with areas of 1.766 cm^2 were punched out and vacuum dried at 120 °C for 4 h in a B-585 Büchi Glass oven. The electrodes were then transferred into an argon-filled MBraun Labstar glove box (H_2O and O_2 content <1 ppm) for half-cells assembly. The final mass loading of the dried LFP electrodes ranged from 2.8 to 3.2 mg cm^{-2} for the 80:10:20 slurry and from 5.7 to 8 mg cm^{-2} for the 92:5:3 slurry. Finally, 2032-type coin cells were assembled by using lithium disks (Ø 16 mm, 0.6 mm thick, high purity lithium chips from Tobmachine), a glass fiber separator (18 mm diameter, 0.26 mm thickness, Whatman), and 100 μL of 1 M lithium hexafluorophosphate in 1:1 v/v mixture of ethyl carbonate and dimethyl carbonate (Solvionic). To preserve the intrinsic porosity of the electrodes and minimize potential limitations related to electrolyte infiltration and lithium-ion transport, the materials were deliberately not subjected to pressing or

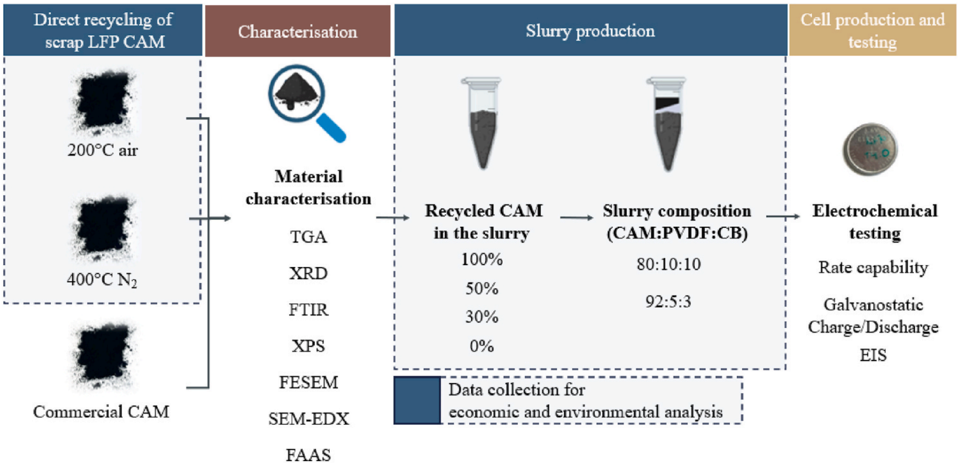

Fig. 1. Experimental process flow of the study (TGA: thermogravimetric analysis; XRD: X-ray diffraction spectroscopy; FTIR: Fourier transform infrared spectroscopy; XPS: X-ray Photoelectron Spectroscopy; FESEM: field emission scanning electron microscopy; SEM-EDX: Scanning Electron Microscopy - Energy Dispersive X-ray Spectroscopy; FAAS: Flame Atomic Absorption Spectroscopy; CAM: cathode active material; PVDF: polyvinylidene fluoride; CB: Carbon Black; EIS: electrochemical impedance spectroscopy).

calendaring. For comparison purposes, cells including cathodes containing only commercial LFP CAM were also fabricated and tested as reference for both slurry compositions (80:10:10 and 92:5:3). Two cells were manufactured for each slurry composition and considering variable contents of recycled CAM.

2.4. *Electrochemical testing*

Electrochemical characterisation of the manufactured cells was carried out in an Arbin BT-2000 battery tester at room temperature in the voltage range between 2.4 V and 3.8 V vs Li/Li^+. The rate capability of the cells was evaluated by applying different current regimes from C/10 to C/5, C/2, 1C to C/10, assuming a theoretical specific capacity of 170 mAh g^{-1} [33,34]. Subsequently galvanostatic cycling was conducted at a C/5 rate. Finally, long term stability was investigated with galvanostatic cycling at a 2C rate for 220 cycles.

Electrochemical impedance spectroscopy (EIS) measurements were carried out by a versatile multichannel potentiostat (VMP-3 Biologic). Impedance measurements were performed before and after three galvanostatic charge-discharge cycles at C/10 using an amplitude of 10 mV in the frequency range of 100 kHz to 10 mHz. For the cell before cycling, all the Nyquist plots consist of one semicircle followed by a straight diffusion line from the high to low frequency regions. The impedance plots were fitted using ZView software.

2.5. *Economic and environmental analyses*

The economic and environmental impacts of integrating low-temperature direct recycling of production scraps into LFP cell manufacturing were evaluated aiming at comparing costs and greenhouse gas (GHG) emissions for different slurry compositions and amounts of recycled CAM included in the slurry. The cost and environmental analyses involved a gate-to-gate system, i.e. the specific focus was on slurry production, and 1 kg of slurry was considered as functional unit. The full details and results on the economic and environmental analyses of direct recycling process applied to LFP and NMC scrap cathodes at different temperatures and in air or N_2 are in the mentioned previous study [30]. This study considers only the data related to the direct recycling conditions 200 °C air and 400 °C N_2 (Table 1), while the data referred to commercial materials were retrieved from literature (Supplementary materials Table S1 and Supplementary materials Table S2). Economic and environmental analysis was only conducted to conditions analysed in the electrochemical part of the study. In the calculations NMP recovery rate was set to 96% [35].

To evaluate the threshold for economic viability of studied on-site scrap recycling strategy, a sensitivity analysis was performed. Currently, many battery manufacturers establish external recycling agreements for scrap material management [6]. Assessing the precise value of LFP production scrap in this context is challenging because of the lack of public data and significant regional disparities. In Europe, LFP scrap recycling is not currently market-driven [38] for example due to recent decrease in lithium prices and inefficient recycling methods [8,39]. Conversely, in China, recycling of LFP, particularly materials with higher lithium content and low degradation level, remains more profitable due to lower operational costs, extensive industrial experience and governmental support, creating a viable market value for LFP production scraps [8,40].

Table 1
Parameters used for the economic and environmental analyses (CAM: cathode active material, PVDF: Polyvinylidene fluoride, NMP: N-Methyl-2-pyrrolidone, GHG: Greenhouse gas).

Pristine Material	Cost (€/kg)	Reference	GHG emissions ($kgCO_2/kg$)	Reference
Commercial CAM	8.8	[36]	8.57	[36]
PVDF	11.15	[36]	2.08	[36]
Carbon Black	4.4	[36]	1.6	[37]
NMP	1.8	[36]	4.61	[36]
Recycled CAM				
200 °C air	0.71	[30]	1.18	[30]
400 °C N_2	2.36	[30]	2.02	[30]

Given these uncertainties in scrap value, this proof-of-concept sensitivity analysis focused on slurry material costs (excluding capital investment and operational expenses) for the 92:5:3 slurry composition in European context. Two scenarios were compared:

Scenario 1 (Baseline): 100% virgin materials, while production scrap is sold to external recyclers. The profit of selling the scrap material is reduced from the material costs.

Scenario 2 (On-site integration): The maximum reported industrial scrap rate 30% is assumed. This material is directly recycled with the 200 °C air treatment method and the remaining 70% of the material is purchased from external sources at current market prices [41].

3. Results and discussion

3.1. *Materials characterization*

The residual PVDF content in pristine LFP scrap CAM and in the recycled materials was quantified through TGA. Within the applied temperature range and inert atmosphere, neither carbon black nor LFP is expected to decompose [42,43]. Therefore, the observed weight loss is primarily due to PVDF decomposition [42].

The pristine LFP scrap (Fig. 2A) demonstrated a 4.9% total mass loss, consistent with the manufacturer's declared composition. The mass loss observed at low temperatures corresponds to the evaporation of moisture absorbed by the material during storage. The 200 °C air material (Fig. 2B) exhibited a similar loss of 4.1%-wt and the slight deviations in the decomposition profile likely result from partial PVDF structural alterations during thermal treatment [44]. In contrast, the 400 °C N_2 material (Fig. 2C) showed a significantly reduced mass loss of 2.1%-wt, indicating more effective binder removal during recycling.

Minimising PVDF content is generally desired in battery recycling, as it is reported to improve the electrochemical performance of recycled cathode active material [13,45,46]. It should be noted that existing literature focuses on spent battery materials, where PVDF is often already degraded during battery use, and binder residuals can decrease the efficiency of metallurgical recycling [24,47]. PVDF decomposition at high temperatures also implies the release of HF, which is hazardous and causes structural changes on the surface of active material [46]. Nonetheless, a few studies dedicated to direct recycling of cathode production scraps have demonstrated that good electrochemical performance can still be achieved even in the presence of residual PVDF, with Wagner et al. reporting 2%-wt residual binder content [4,48,49]. Based on the contents of residual PVDF detected in the recycled materials, calculations were made to determine how much pristine PVDF needs to be added during subsequent slurry production to achieve the desired binder content (Supplementary materials Table S3).

To enable direct reintegration of recycled materials into slurry preparation, the CAM crystalline structure must remain intact during direct recycling. For LFP, a key degradation pathway at elevated temperatures is the oxidation of $LiFePO_4$ to $Li_3Fe_2(PO_4)_3$ and Fe_2O_3, which compromises electrochemical performance [50]. The XRD spectra of LFP scrap material and recycled CAM samples (Fig. 3) are consistent with a single-phase olivine $LiFePO_4$ structure with an orthorhombic unit cell, and no secondary phases are observed in any of the recycled samples. This confirms that nitrogen atmosphere effectively prevents LFP oxidation even at higher temperatures.

FTIR analysis was initially employed to further investigate PVDF degradation but the low binder content in the samples prevented accurate analysis (Supplementary materials Fig. S1). XPS analysis was then conducted to assess the chemical state of CAM surface after the

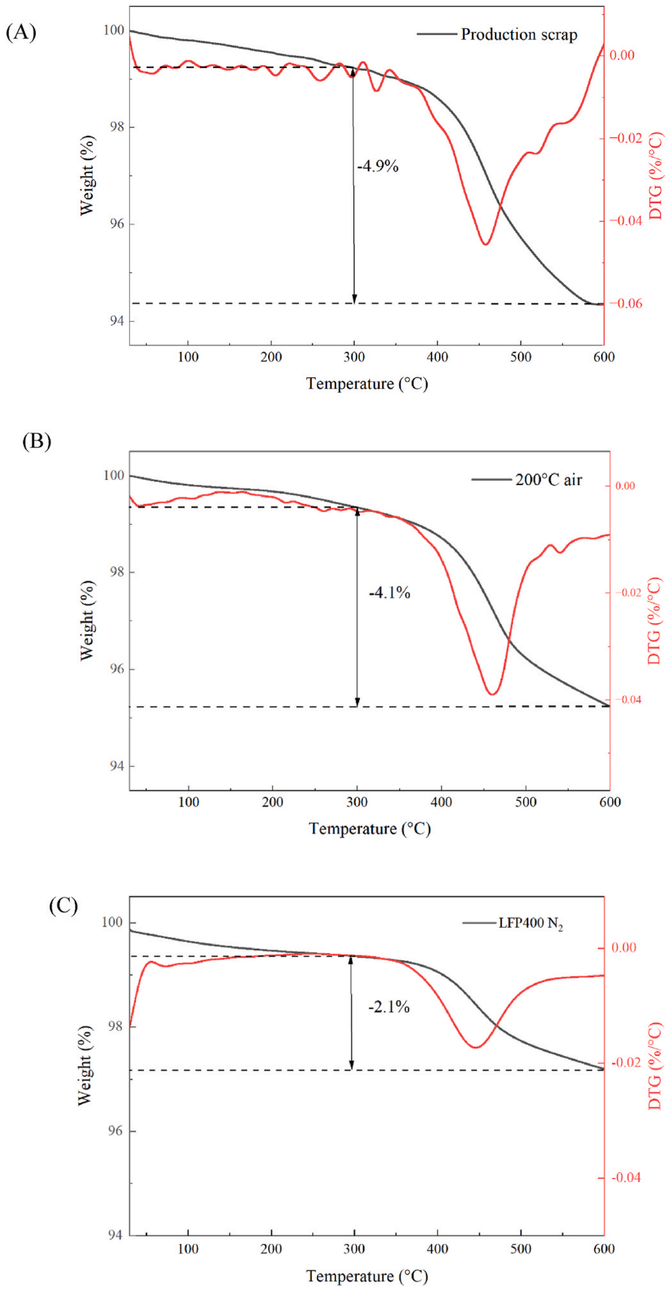

Fig. 2. Results on thermogravimetric analysis of (A) pristine LFP scrap, (B) 200 °C air and (C) 400 °C N_2 CAM (DTG: derivative thermogravimetric curves).

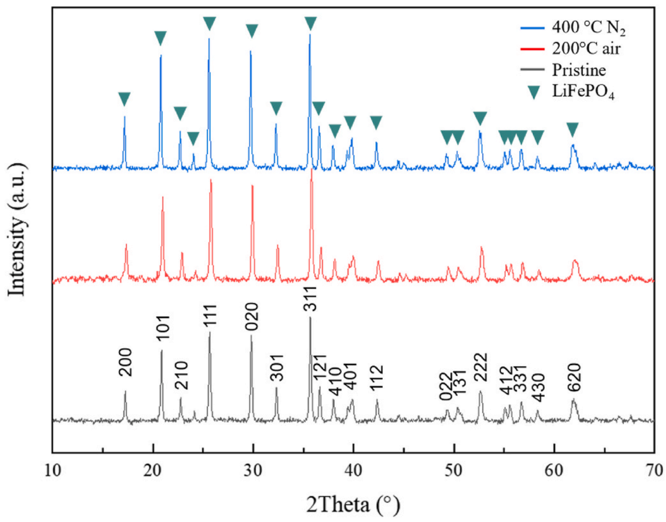

Fig. 3. XRD spectra of pristine LFP scrap, 200 °C air and 400 °C N_2 CAM.

studied recycling conditions compared to the pristine reference material (Fig. 4; atomic concentration in Supplementary materials Table S5). PVDF degradation in 400 °C N_2 is revealed by reduction of characteristic CF_2-CH_2 bonds by 45.5% at 290.8 eV (Figs. 4A) and 7.4% decreases at 687.9 eV (Fig. 4C) compared to the pristine reference material [48]. Simultaneously, bonds associated to carbon black change their state from sp^2 (284.6 eV) to sp^3 (285.1 eV) indicating possible longer carbon chain formation after fluorine detaching from PVDF structure. The concentration of C-O and C=O bonds at 287.5 eV and 288.7 eV also increase in the 400 °C N_2 samples which can indicate breakage of C-F and C-H bonds from PVDF, loss of hydrogen and fluorine and redistribution of electrons [51]. The O1s peak (Fig. 4B) also reveals an increase in C-O bond concentration at 533.4 eV. The total atomic concentration of fluorine is reduced by 43% after treatment in 400 °C in nitrogen. While some of the liberated fluorine reacts with the active material surface forming $Li_xPO_yF_z$, evidenced by the increase in peaks at 689.4 eV (Fig. 4C) and at 134.8 eV (Fig. 4D), some fluorine leaves the system with the processing gas flow. In contrast, these above-mentioned changes are not significant in 200 °C air samples validating that only small part of PVDF degraded in this condition. Importantly, LiF and Fe-F bonds' formation is minimal, and the Fe valence state stays intact throughout the studied conditions. This preservation of Fe state is presented in Fig. 4F where Fe 2p spectra indicate no changes in Fe $2p_{3/2}$ peak at 710 eV, satellite peak around 715 eV or Fe$2p_{1/2}$ peak at 724 eV [52]. This is consistent with the XRD results, which indicate that the Fe oxidation state remains unchanged after low-temperature thermal treatments.

FESEM analysis (Supplementary materials Fig. S2) confirms that direct recycling preserves the physical integrity and surface morphology of the $LiFePO_4$ particles. Both the 200 °C air and 400 °C N_2 samples exhibit particle size distributions comparable to the pristine material, with limited grain growth. In addition, carbon black particles remain visible on all surfaces. On the other hand, SEM-EDX illustrates more localized fluorine and carbon region in the recycled materials without clear differences between the 200 °C and 400 °C N_2 samples (Fig. 5). However, carbon clustering interpretation is limited by possible background interference from the carbon tape used in the sample preparation. Despite this slight elemental inhomogeneity, no severe particle agglomeration is evident. Notable, tighter particle size control could be achieved during scale-up via additional milling or finer sieving. Finally, elemental analysis confirms that aluminium impurities remain minimal following thermal treatment and mechanical separation (Supplementary Table S4).

3.2. *Electrochemical testing*

The electrochemical tests involved coin cells manufactured using two slurry formulations: an initial laboratory-scale formulation (80:10:10) and an industrially relevant formulation (92:5:3). For the 80:10:10 slurry, cells were first prepared with 100% recycled CAM treated either at 200 °C in air or 400 °C in N_2, to evaluate the standalone performance of the materials. Based on these results, recycled CAM was blended with commercial CAM at 50%, and 30%-wt to identify the maximum recycled content that maintained electrochemical performance comparable to that of fully commercial material. This maximum recycled CAM content was tested in the 92:5:3 slurry composition to evaluate its applicability under industrially relevant conditions.

3.2.1. *Performance of cells based on 80:10:10 slurry including 100%-wt of recycled CAM*

When dosed as 100% of CAM in the slurry, the material recycled at

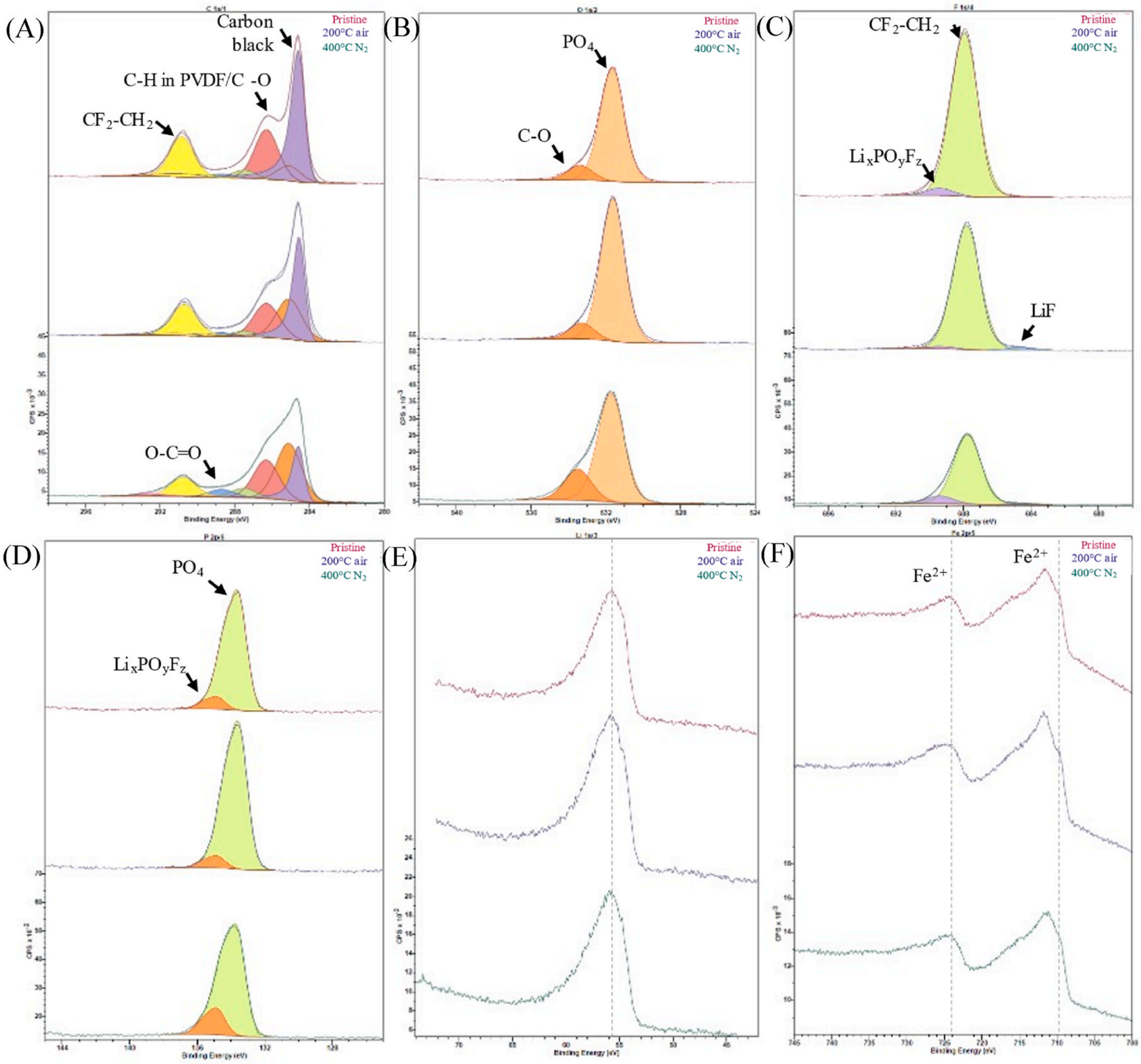

Fig. 4. XPS (A) C1s (B) O1s (C) F1s (D) P2p (E) Li1s (F) Fe2p spectras of pristine LFP scrap, 200 °C air and 400 °C N_2 CAM.

400 °C in N_2 exhibited a rate capability closely matching that of the commercial CAM (Fig. 6 and Supplementary materials Fig. S4). At a C/10 rate, initial discharge capacities of 153 mAh g^{-1} and 155 mAh g^{-1} were recorded for the 400 °C N_2-treated CAM and the commercial material, respectively. At a higher rate of 1C, these values were 138 mAh g^{-1} and 136 mAh g^{-1} and after a subsequent 50 cycles at C/5, both materials maintained a capacity of 148 mAh g^{-1} (Fig. 6B). To assess long-term stability, extended cycling was performed at 2C rate. The 400 °C N_2 electrode exhibited high coulombic efficiency (>98%) and capacity retentions of 96% measured from the 10th cycle up to 220 cycles (Supplementary materials Fig. S5). These results suggest that direct recycling at 400 °C in N_2 preserves the electrochemical performance of the LFP cathode production scraps even with 2.1%-wt residual PVDF binder.

In contrast, the electrodes with 100% of CAM recycled at 200 °C displayed a stable cycling profile, but with lower initial capacity (−8%) compared to 400 °C N_2 and the commercial CAM (Fig. 6A). The initial discharge capacity of 153 mAh g^{-1} was recorded for 200 °C CAM at C/10, while at 1C the capacity was 123 mAh g^{-1} and after 50 cycles of galvanostatic cycling at C/5 the capacity remained at 136 mAh g^{-1} (Fig. 6B). After 220 cycles the coulombic efficiency remained high at 99% and capacity retention was measured to be 95% (Supplementary materials Fig. S5). All in all, these findings indicate that a higher concentration (i.e. 4.1%-wt) of residual PVDF may have a negative impact on the electrochemical performance. Similar results were also reported previously [29], comparing direct recycling of NMC111 production scraps through mechanical and chemical solvent-based separation methods leading to different residual PVDF concentrations. An explanation of such effect of recycling can be the alteration in the PVDF crystalline structure during thermal treatment, which results in lower adhesion to the current collector which decreases electrical and ionic conductivity [44,53], even at low temperatures (160 °C) [54]. A decrease in electrochemical performance of recycled active materials with high residual binder is also associated with material pore clogging due to residual carbon black and binder [48]. Residual PVDF is known to reduce the electrode material tap density, thereby lowering the cell energy density [46].

Conductivity of the electrodes were studied by Electrochemical Impedance spectroscopy. The resulting Nyquist plots were modelled using Z-View software based on the simplified equivalent circuit (Supplementary materials Fig. S3). In this model, the intercept of the semicircle with the real axis (−Z″) represents the solution resistance (Rs), while the diameter of the semicircle corresponds to the charge-transfer resistance (Rct). The sloping linear region at lower frequencies is attributed to lithium-ion diffusion and was fitted using a Warburg impedance (Zw) element. After cycling, the optimal fit was achieved

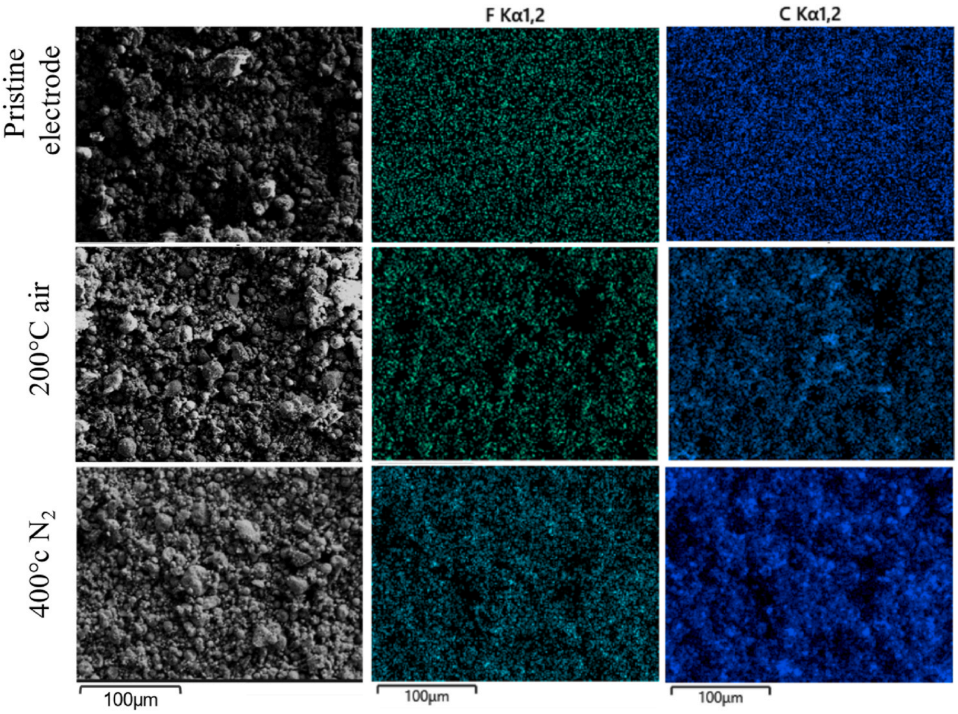

Fig. 5. SEM-EDX of fluorine and carbon in pristine LFP scrap, 200 °C air and 400 °C N_2 CAM.

with an equivalent circuit (R1 + R2/CPE1 + R3/CPE2). As evidenced by the EIS analysis, the Rtc values are essentially similar for cells employing LFP treated at 400 °C under N_2 and those based on commercial LFP, both fabricated with an 80:10:10 electrode composition. This close agreement is consistent with the similar electrochemical response exhibited by the cells during galvanostatic charge–discharge cycling. In contrast, cells containing LFP treated at 200 °C in air display a substantial increase in charge-transfer resistance, indicative of hindered interfacial charge-transfer kinetics.

3.2.2. Performance of cells based on 80:10:10 slurry including 30 and 50%-wt of recycled CAM

For the material recycled at 400 °C N_2, a 100% recycled content exhibited electrochemical performance similar to the commercial reference. A further reduction in recycled content was deemed unnecessary. While it is reasonable to assume that lower concentrations would also preserve high electrochemical performance, this assumption was not experimentally verified in the present study.

The 200 °C air CAM exhibited lower performance when used at 100% content. To address this limitation, a blend of 50% recycled and 50% commercial material was produced keeping the composition at 80:10:10. As presented in Fig. 7A, this blend improved performance compared to the 100% recycled material, with initial discharge capacity of 153 mAh g^{-1} at C/10 and 130 mAh g^{-1} capacity at 1C. The 50% 200 °C air electrode still exhibited a lower capacity compared to the commercial with a capacity retention of 95% after 50 cycles. In addition, the cells suffered a low coulombic efficiency (Supplementary materials Fig. S7).

A further reduction to 30% recycled content yielded electrode performance comparable to reference commercial cells with an initial discharge capacity of 154 mAh g^{-1} and 137 mAh g^{-1} at 1C as well as capacity retention of 98% after 50 cycles suggesting that incorporating up to 30% of 200 °C air material is a viable limit without significant loss in electrochemical performance assuring stable cycling performance also in longer cycling tests (Fig. 7B). This 30% threshold aligns with the highest scrap rate reported for battery production lines [2]. This finding suggests that all scrap material generated during production could potentially be reintegrated into the slurry preparation process either through direct recycling via low-temperature 200 °C air treatment or 400 °C N_2 treatment without compromising cell performance when 80:10:10 composition is used.

3.2.3. Performance of cells based on 92:5:3 slurry including 100 and 30%-wt recycled CAM

The slurry composition was changed to an industrially more relevant composition of 92:5:3 while maintaining the concentration for recycled material as defined above. 30% 200 °C air CAM reached performance comparable to commercial material, with initial discharge capacity of 154 mAh g^{-1} and 133 mAh g^{-1} at 1C (Supplementary materials Fig. S10 and Supplementary materials Fig. S11). However, cells with 100% 400 °C N_2 active material exhibited lower performance with an initial discharge capacity of 140 mAh g^{-1} and 121 mAh g^{-1} at 1C indicating that with higher active material loadings, the proportion of recycled content should be reduced - ideally aligning with the actual scrap rates observed in battery manufacturing. The measured lower performance of 100% 400 °C N_2, could be due to reduced electrical conductivity, as conductive carbon content in this composition is low and no additional pristine carbon black was added to the slurry. The PVDF residual was implied in SEM-EDX (Fig. 5) analysis to cause modest carbon black agglomeration and the processing steps used in this study might not have been adequate to avoid these agglomerations and produce a uniform LFP-carbon black particles interconnection. This might result in insufficient electronic conductivity in some areas of the electrode. Formation of inactive $Li_xPO_yF_z$ on 400 °C N_2 samples as detected in XPS analysis can also reduce the cell performance in cells with high active material concentration. In addition, it is worth noting that due to the limited quantity of production scrap raw material, no calendaring step was performed which can affect the cell performance [55]. However, all cells were prepared following the same laboratory scale electrode production method described earlier.

3.3. Economic and environmental analysis

Fig. 8A presents a comparative cost analysis associated to the

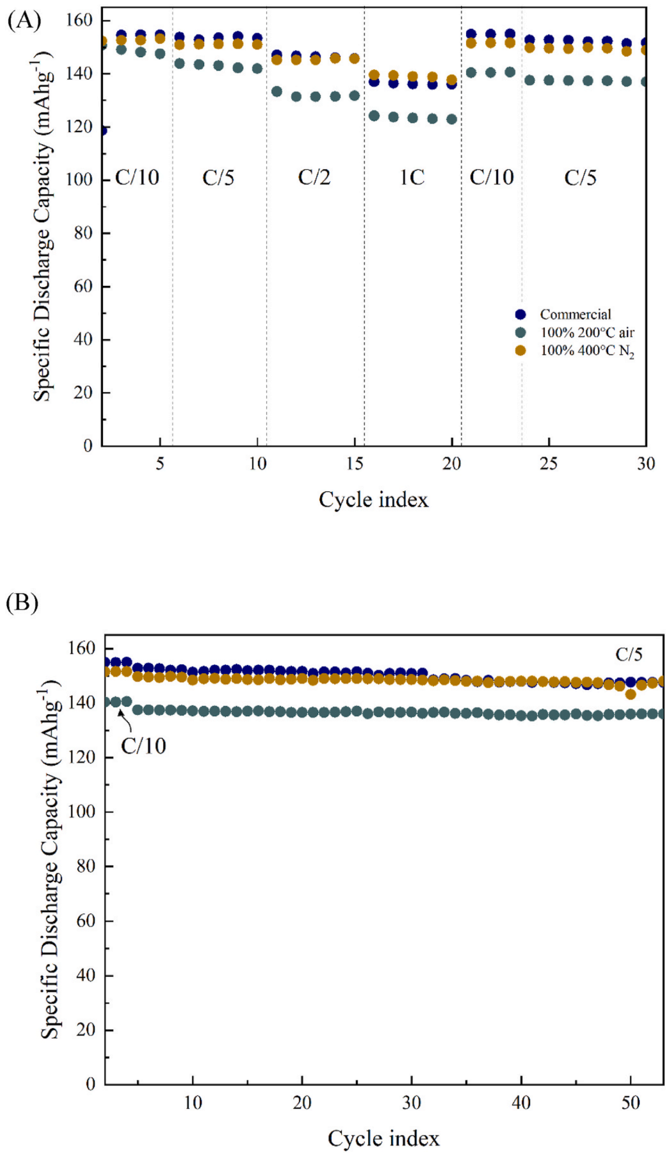

Fig. 6. Rate capability test (A) and Cycling performance (B) of 100% commercial and 100% recycled LFP electrodes with 80%-wt CAM: 10%-wt binder:10%-wt carbon black composition.

preparation of 1 kg of slurry considering the two studied compositions (80:10:10 and 92:5:3) with studied blends of recycled and commercial CAM. The results indicate that integrating recycled CAM is economically beneficial under all evaluated conditions. The 92:5:3 formulation consistently exhibits a lower total cost than the 80:10:10 formulation, primarily because the low cost of LFP, especially recycled CAM, offsets the high cost of virgin PVDF required for the binder-rich composition.

Baseline costs for slurries using 100% virgin materials were calculated at as 9.21€/kg_{Slurry} and 9.06 €/kg_{Slurry} for 80:10:10 and 92:5:3 compositions, respectively. Introducing 100% recycled CAM in the slurry reduced theses values significantly to 2.06 €/kg_{Slurry} and 0.83 €/kg_{Slurry} with 200 °C air. Utlizing 100% 400 °C N_2 CAM resulted slightly higher cost of 3.77 €/kg_{Slurry} and 2.80 €/kg_{Slurry} due to increased energy demand, nitrogen consumption, and the need for additional virgin binder to compensate for greater PVDF degradation during thermal treatment. While reducing the recycled content improves electrochemical performance, it also increases material costs. For the 200 °C air material, a 50%-wt blending with commercial material resulted in costs of 5.64 €/kg_{Slurry} (80:10:10) and 4.95 €/kg_{Slurry} (92:5:3) while

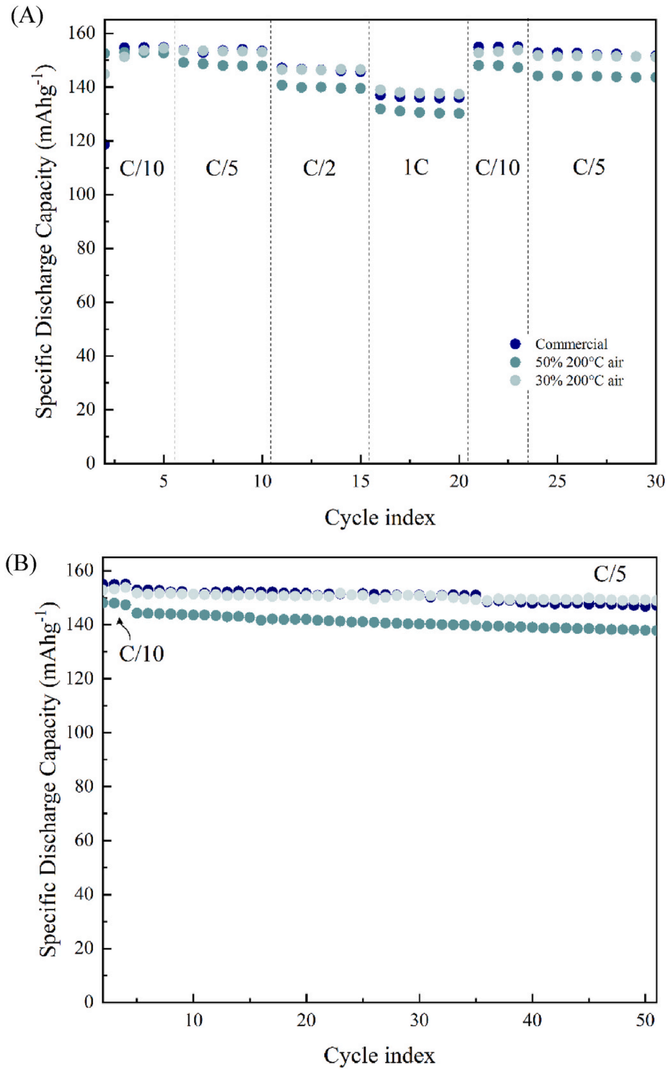

Fig. 7. Rate capability test (A) and Cycling performance (B) of reference 100% commercial electrodes and 200 °C air electrodes with 50% and 30% recycled material with 80%-wt CAM: 10%-wt binder:10%-wt carbon black composition.

lowering the recycled content further to 30%-wt increased costs to 7.07 €/kg_{Slurry} and 6.59 €/kg_{Slurry}. However, even at this 30% substitution level, the total slurry cost remains 23% and 28% lower than the virgin baseline for the 80:10:10 and 92:5:3 compositions, respectively.

Based on the slurry costs from the economic analysis, a sensitivity analysis was conducted to account for material price volatility. These results indicate that on-site direct recycling using 30% 200 °C air CAM is economically superior to external recycling if the market value of LFP production scrap remains below ~2.5 €/kg (Supplementary materials Fig. S12A). The economic advantage of on-site recycling increases with higher virgin LFP prices but it diminishes if virgin prices fall or if the market value of scrap rises (Supplementary materials Fig. S12B). Currently, the low value of LFP scrap in Europe makes on-site recycling highly viable, even though future market maturation could narrow this cost advantage.

GHG analysis (Fig. 8B) confirms that replacing virgin LFP CAM with recycled material significantly reduces the environmental impact of slurry materials, driven by the high carbon intensity of virgin production versus the minimal footprint of on-site recycling. The GHG emissions associated to virgin material slurry were 7.68 and 8.27 $kgCO_2/kg_{Slurry}$ for 80:10:10 and 92:5:3 compositions respectively but introducing 100% 200 °C air CAM lowered these values to 1.72 and 1.41 $kgCO_2/$

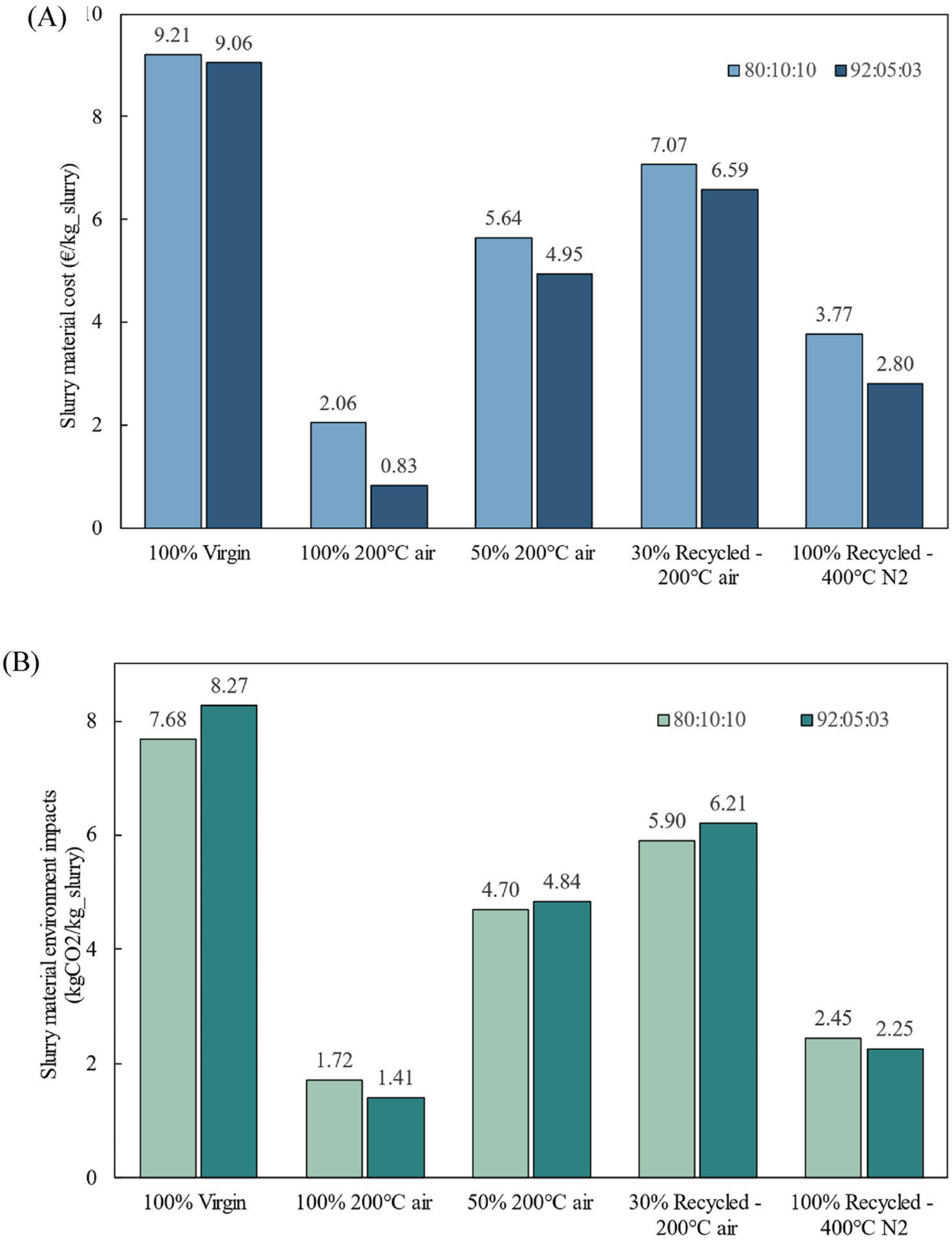

Fig. 8. Slurry material (A) cost and (B) environmental impact for 80:10:10 and 92:5:3 compositions using virgin LFP, 100% recycled CAM, and blends of recycled and virgin CAM.

kg_{Slurry}. Slurry based on 100% 400 °C N_2 CAM indicated slightly higher emissions (2.45 and 2.25 $kgCO_2/kg_{Slurry}$) remaining still superior to virgin material slurries. This analysis also highlighted that even partial substitution with recycled material leads to reductions in GHG emissions compared to the exclusive utilisation of virgin CAM. As the GHG emissions associated with on-site direct recycling of LFP production scrap are minimal, the recycled material appears not only cost-effective but also environmentally advantageous.

4. Discussion

The findings of this study were benchmarked against state-of-the-art studies on Li-ion battery production scrap recycling (Table 2), revealing that short-loop reintegration strategies remain largely at the proof-of-concept stage. The methodology for electrochemical testing employed here is consistent with the current literature, where initial material performance is typically assessed over a limited number of cycles, as the majority of reviewed studies either omit electrochemical performance or limit testing to 200 cycles or fewer.

However, Table 2 also highlights critical guidelines for future research on recycling of production scraps where the aim should be at moving from preliminary lab scale studies to industrially scalable processes. More holistic diagnostic techniques are required to fully understand the quality of recycled materials. Notably, advanced characterization remains scarce in current literature, as only three other studies included XPS analysis, one other study incorporated EIS and two utilizing cyclic voltammetry (CV). Moreover, while technical durability is essential, industrial scalability cannot be assessed without critical economic and environmental validation. Currently, only four of the reviewed studies on production scrap recycling included assessment of economic and environmental impacts.

As upcoming EU regulations will require reporting of battery carbon footprint and the incorporation of recycled materials into cell manufacturing, more studies are needed to address these regulatory

Table 2

Comparison of the present study with state-of-the-art literature on Li-ion battery production scrap recycling. (NMP: N-Methyl-2-pyrrolidone, CV: Cyclic voltammetry, EIS: Electrochemical impedance spectroscopy, XPS: X-ray Photoelectron Spectroscopy, PVDF: Polyvinylidene difluoride, CMC: Carboxymethyl cellulose, TRD: fluorine acrylic hybrid latex).

Ref.	Scrap Chemistry	Recycling strategy	Specific Discharge Capacity (mAh/g) *Residual binder present	Residual binder in cells	Tested Cycles	CV	Rate capability	EIS	Emission	Economic
This study	LFP	Thermomechanical	154*	PVDF	220	-	✓	✓	6.21 kg CO2/kg slurry	6.59 €/kg slurry
[21]	LFP	Thermomechanical	-	-	-	-	-	-	3.33 kgCO2 eq/kg detached	1.45€/kg detached
[56]	LFP	Leaching	-	-	-	-	-	-	-	2.24 €/kg
[57]	LNMO	Thermal and ice-striping	135*	CMC, TRD	100	-	✓	-	-	-
[18]	NMC 811	Thermomechanical	-	-	-	-	-	-	-	-
[28]	NMC111	Thermomechanical	115	-	500	-	-	-	-	-
[24]	NMC111	Thermal and Chemical	147*	PVDF	75	-	-	-	-	-
[4]	NMC111	Thermal and Chemical	157.8, 136*	PVDF	200	✓	✓	-	-	-
[29]	NMC111	Mechanical and Chemical	125*	PVDF	500	-	-	-	-	-
[58]	NMC532	Thermal	164	-	50	-	-	-	-	-
[59]	NMC532	Solid-state sintering	155.7	-	100	-	-	-	-	-
[60]	NMC622	Chemical	164*	PVDF	100	-	✓	-	-	-
[49]	NMC622	Chemical	160	PVDF	18	✓	✓	-	-	-
[12]	NMC622	Chemical	158	-	40	-	-	-	-	-
[48]	NMC811	Thermal (Induction)	208*	PVDF	21	-	✓	✓	-	-
[61]	NMC811	Thermal (Induction)	.	-	-	-	-	-	-	-
[62]	NMC831205	Dry-mechanical	205.7*	PTFE	32	-	✓	-	Benefit 0.02 kgCO2/kWh	Savings 0.8 $/kWh
[63]	Graphite	Mild leaching and Thermal	357.1	-	1	-	-	-	3.2 kgCO2/kg metals recovered	-

demands. Recycling approaches must achieve an appropriate balance between cost and performance, and strategies for implementing recycled materials in industrial production should be systematically studied and critically evaluated. The present study found that minimal preprocessing of low value LFP production scraps, followed by blending with pristine material, delivers promising technical performance of produced electrodes while reducing costs and environmental impacts, aligning with anticipated industrial requirements.

5. Conclusions

This study examined strategies for integrating on-site low-temperature direct recycling of LFP production scrap cathodes into battery cell production. Characterization confirmed that direct recycling at 200 °C in air retained the CAM properties similar to pristine material whereas treatment at 400 °C in nitrogen caused higher PVDF degradation leading to formation of LixPOyFz on the material surface.

Electrochemical testing demonstrated that residual PVDF had a limited impact on cell performance. CAM recycled at 200 °C in air with industrially relevant slurry composition (92:5:3) delivered good performance of 154 mAh g^{-1} when the recycled material content was limited to 30%. Meanwhile, scrap recycled at 400 °C in N_2 maintained its electrochemical performance of 154 mAh g^{-1} with 100% recycled content in the 80:10:10 slurry. However, with the higher active material content composition in the 92:5:3 slurry, the discharge capacity of 100% 400 °C N_2 cells dropped to 140 $mAhg^{-1}$.

Economic analysis indicated that low-temperature direct recycling of production scraps reduces the slurry material cost significantly. For the lower active material composition (80:10:10), material costs decreased to 7.07 €/kg including 30% recycled 200 °C material, and to 3.77 €/kg with 100% 400 °C N_2 recycled material. Even with higher active material composition (92:5:3), slurry costs for recycled material (6.59 €/kg for 30% 200 °C air and 2.80 €/kg for 400 °C N2) remained below those of slurries based on virgin material (9.06 €/kg). Sensitivity analysis confirmed that 30% integration of 200 °C recycled material for production of higher active material content slurry, remains economically viable if the market price for LFP scrap stay below 2.5 €/kg, and virgin LFP prices do not decline substantially.

Environmental impact analysis revealed similar results with GHG emissions reduction to 5.90 and 2.45 kg CO_2/kg for 30% 200 °C and 100% 400 °C N_2 recycled materials, compared to 7.68 kg CO_2/kg for pristine active material with low CAM composition. With higher CAM composition, emissions were 6.21 and 2.25 kg CO_2/kg for 200 °C air and 400 °C N2, respectively, again lower than for virgin material.

In conclusion, reintegrating scrap cathodes into production supports the circular economy, reduces costs and emissions, and enhances the supply chain security of local battery manufacturing while maintaining good electrochemical performance. Future research should focus on optimizing the direct recycling process to improve the material technical performance to meet the excellent economic and environmental quality. Scaling up direct recycling will also require larger material batches and more advanced manufacturing steps, including improved particle size control and calendaring steps.

CRediT authorship contribution statement

Lotta Liina Lassila: Writing – original draft, Visualization, Methodology, Investigation, Formal analysis, Data curation. **Martina Bruno:** Visualization, Methodology, Investigation. **Carlotta Francia:** Writing – review & editing, Supervision, Methodology, Formal analysis, Conceptualization. **Annukka Santasalo-Aarnio:** Writing – review & editing, Supervision, Methodology, Conceptualization. **Matteo Gandolfo:** Writing – review & editing, Formal analysis, Data curation. **Silvia Fiore:** Writing – review & editing, Validation, Supervision, Methodology, Funding acquisition, Conceptualization.

Declaration of competing interest

The authors declare that they have no known competing financial interests or personal relationships that could have appeared to influence the work reported in this paper.

Acknowledgements

This study was carried out within the project “Dipartimenti di Eccellenza 2023-2027 (l. 232/2016, art. 1, - commi 314 - 337)” - Department of Environment, Land and Infrastructure Engineering of Politecnico di Torino – funded by Ministero dell’Università e della Ricerca. This manuscript reflects only the authors' views and opinions, and the Ministry cannot be considered responsible for them. The authors gratefully acknowledge the National Research and Development Institute for Cryogenic and Isotopic Technologies – ICSI Rm. Valcea, in Romania for providing the scrap cathodes.

Appendix A. Supplementary data

Supplementary data to this article can be found online at https://doi.org/10.1016/j.jpowsour.2026.239558.

Data availability

Data will be made available on request.

References

[1] International Energy Agency (IEA), Global EV outlook 2025 expanding sales in diverse markets [Online]. Available: www.iea.org, 2025. (Accessed 13 June 2025).
[2] L. Gaines, J. Zhang, X. He, J. Bouchard, H.E. Melin, Tracking flows of end-of-life battery materials and manufacturing scrap, Batteries 9 (7) (Jul. 2023) 360, https://doi.org/10.3390/BATTERIES9070360/S1.
[3] Fraunhofer Research Institution for Battery Cell Production FFB, Mastering Ramp-up of Battery Production, 2024.
[4] X. Zhang, Q. Xue, L. Li, E. Fan, F. Wu, R. Chen, Sustainable recycling and regeneration of cathode scraps from industrial production of lithium-ion batteries, ACS Sustain. Chem. Eng. 4 (12) (Dec. 2016) 7041–7049, https://doi.org/10.1021/acssuschemeng.6b01948.
[5] E. Mossali, N. Picone, L. Gentilini, O. Rodrìguez, J.M. Pérez, M. Colledani, Lithium-ion batteries towards circular economy: a literature review of opportunities and issues of recycling treatments, J. Environ. Manag. 264 (Jun. 2020) 110500, https://doi.org/10.1016/J.JENVMAN.2020.110500.
[6] L. Gaines, Q. Dai, J.T. Vaughey, S. Gillard, Direct recycling R&D at the ReCell center, Recycling 6 (2) (2021), https://doi.org/10.3390/recycling6020031.
[7] P. Xu, Q. Dai, H. Gao, L. Gaines, J. Lu, Z. Chen, Efficient direct recycling of lithium-ion battery cathodes by targeted healing, Joule 4 (12) (2020) 2609–2626, https://doi.org/10.1016/j.joule.2020.10.008.
[8] Transport & Environment, From waste to value: the potential for battery recycling in Europe [Online]. Available: https://www.transportenvironment.org/articles/from-waste-to-value-the-potential-for-battery-recycling-in-europe, 2024. (Accessed 7 July 2025).
[9] European Commission, Updated List of European Waste with battery-related waste codes | environment [Online]. Available: https://environment.ec.europa.eu/document/48cdc11b-facb-429a-80ad-4b37bce77ced_en. (Accessed 13 June 2025).
[10] The European Union, REGULATION (EU) 2023/1542 of the European Parliament and of the Council of 12 July 2023 concerning batteries and waste batteries, amending Directive 2008/98/EC and Regulation (EU) 2019/1020 and repealing Directive 2006/66/EC [Online]. Available: https://eur-lex.europa.eu/legal-content/EN/TXT/?uri=CELEX:32023R1542, 2023. (Accessed 13 June 2025).
[11] N. Hayagan, et al., Challenges and perspectives for direct recycling of electrode scraps and end-of-life lithium-ion batteries, Batter. Supercaps 7 (6) (Jun. 2024) e202400120, https://doi.org/10.1002/BATT.202400120.
[12] Y. Bai, W.B. Hawley, C.J. Jafta, N. Muralidharan, B.J. Polzin, I. Belharouak, Sustainable recycling of cathode scraps via Cyrene-based separation, Sustain. Mater. Technol. 25 (Sep. 2020) e00202, https://doi.org/10.1016/J.SUSMAT.2020.E00202.
[13] M.S.A. Bhuyan, H. Shin, Green recovery of cathode active materials from Li-Ion battery electrode scraps using propylene carbonate: a novel approach for direct recycling, ACS Sustain. Chem. Eng. 11 (29) (Jul. 2023) 10677–10687, https://doi.org/10.1021/ACSSUSCHEMENG.3C01278.
[14] Y. Bai, N. Muralidharan, J. Li, R. Essehli, I. Belharouak, Sustainable direct recycling of lithium-ion batteries via solvent recovery of electrode materials, ChemSusChem 13 (21) (Nov. 2020) 5664–5670, https://doi.org/10.1002/CSSC.202001479.
[15] W. Lv, Z. Wang, H. Cao, Y. Sun, Y. Zhang, Z. Sun, A critical review and analysis on the recycling of spent lithium-ion batteries, ACS Sustain. Chem. Eng. 6 (2) (Feb. 2018) 1504–1521, https://doi.org/10.1021/acssuschemeng.7b03811.
[16] M. Rahman, M. Hoq, H. Shin, Influence of green solvents on the recovery of cathode active materials from electrode scraps: a comparative study, Electrochim. Acta 508 (Dec. 2024) 145225, https://doi.org/10.1016/J.ELECTACTA.2024.145225.
[17] R. Zheng, et al., Optimized Li and Fe recovery from spent lithium-ion batteries via a solution-precipitation method, RSC Adv. 6 (49) (Apr. 2016) 43613–43625, https://doi.org/10.1039/C6RA05477C.
[18] G. Lombardo, B. Ebin, B.M. Steenari, M. Alemrajabi, I. Karlsson, M. Petranikova, Comparison of the effects of incineration, vacuum pyrolysis and dynamic pyrolysis on the composition of NMC-lithium battery cathode-material production scraps and separation of the current collector, Resour. Conserv. Recycl. 164 (Jan. 2021) 105142, https://doi.org/10.1016/J.RESCONREC.2020.105142.
[19] Q. Sun, et al., Resynthesizing LiFePO4/C materials from the recycled cathode via a green full-solid route, J. Alloys Compd. 818 (Mar. 2020) 153292, https://doi.org/10.1016/J.JALLCOM.2019.153292.
[20] M. Bruno, S. Fiore, Review of upstream processes for Li-ion batteries recycling: safety and economic concerns, J. Clean. Prod. 501 (Apr. 2025) 145327, https://doi.org/10.1016/J.JCLEPRO.2025.145327.
[21] M. Bruno, S. Fiore, Low-cost and environmentally friendly physic-mechanical pre-treatments to recycle lithium iron phosphate cathodes, J. Environ. Chem. Eng. 12 (2) (Apr. 2024) 112106, https://doi.org/10.1016/j.jece.2024.112106.
[22] M. Wang, Q. Tan, L. Liu, J. Li, A Facile, environmentally friendly, and low-temperature approach for decomposition of polyvinylidene fluoride from the cathode electrode of spent lithium-ion batteries, ACS Sustain. Chem. Eng. 7 (15) (Aug. 2019) 12799–12806, https://doi.org/10.1021/acssuschemeng.9b01546.
[23] H. Bi, et al., Low-temperature thermal pretreatment process for recycling inner core of spent lithium iron phosphate batteries, Waste Manag. Res. 39 (1) (Jan. 2021) 146–155, https://doi.org/10.1177/0734242X20957403/ASSET/37EEB8CA-751B-4422-9595-13C985493C69/ASSETS/IMAGES/LARGE/10.1177_0734242X20957403-FIG7.JPG.
[24] D. Song, X. Wang, E. Zhou, P. Hou, F. Guo, L. Zhang, Recovery and heat treatment of the Li(Ni1/3Co1/3Mn1/3)O2 cathode scrap material for lithium ion battery, J. Power Sources 232 (Jun. 2013) 348–352, https://doi.org/10.1016/J.JPOWSOUR.2012.10.072.
[25] G. Yang, Z. Wu, H. Zhu, H. Bi, Y. Bai, L. Wang, Exploration of physical recovery techniques and economic viability for retired lithium nickel cobalt manganese oxide-type lithium-ion power batteries, J. Mater. Cycles Waste Manag. 26 (6) (Nov. 2024) 3571–3583, https://doi.org/10.1007/S10163-024-02061-Y/TABLES/4.
[26] Z. Wu, H. Zhu, H. Bi, P. He, S. Gao, Recycling of electrode materials from spent lithium-ion power batteries via thermal and mechanical treatments, Waste Manag. Res. 39 (4) (Apr. 2021) 607–619, https://doi.org/10.1177/0734242X20969803.
[27] S. Zhou, et al., Direct recovery of scrapped LiFePO4 by a green and low-cost electrochemical re-lithiation method, Green Chem. 24 (16) (Aug. 2022) 6278–6286, https://doi.org/10.1039/D2GC01640K.
[28] C. Hanisch, T. Loellhoeffel, J. Diekmann, K.J. Markley, W. Haselrieder, A. Kwade, Recycling of lithium-ion batteries: a novel method to separate coating and foil of electrodes, J. Clean. Prod. 108 (Dec. 2015) 301–311, https://doi.org/10.1016/J.JCLEPRO.2015.08.026.
[29] C. Hanisch, et al., In-Production recycling of active materials from lithium-ion battery scraps, ECS Trans. 64 (22) (2015), https://doi.org/10.1149/06422.0131ecst.
[30] M. Bruno, L.L. Lassila, C. Francia, A. Santasalo-Aarnio, S. Fiore, Technical, economic and environmental analysis of production scraps direct recycling from lithium-ion battery manufacturing, Clean. Environ. Syst. (Dec. 2025) 100386, https://doi.org/10.1016/J.CESYS.2025.100386.
[31] G. Apachitei, et al., Optimisation of industrially relevant electrode formulations for LFP cathodes in lithium ion cells, Batteries 9 (4) (Apr. 2023) 192, https://doi.org/10.3390/BATTERIES9040192/S1.
[32] D. Versaci, et al., Tailoring cathode materials: a comprehensive study on LNMO/LFP blending for next generation lithium-ion batteries, J. Power Sources 613 (Sep. 2024) 234955, https://doi.org/10.1016/J.JPOWSOUR.2024.234955.
[33] A.K. Padhi, K.S. Nanjundaswamy, J.B. Goodenough, Phospho-olivines as Positive-Electrode materials for rechargeable lithium batteries, J. Electrochem. Soc. 144 (4) (Apr. 1997) 1188–1194, https://doi.org/10.1149/1.1837571/XML.
[34] Z. Ahsan, et al., Recent progress in capacity enhancement of LiFePO4cathode for Li-Ion batteries, J. Electrochem. Energy Convers. Storage 18 (1) (Feb. 2021) 10801–10802, https://doi.org/10.1115/1.4047222/1083876.
[35] D.L. Wood, J.D. Quass, J. Li, S. Ahmed, D. Ventola, C. Daniel, Technical and economic analysis of solvent-based lithium-ion electrode drying with water and NMP, Dry. Technol. 36 (2) (Jan. 2018) 234–244, https://doi.org/10.1080/07373937.2017.1319855.
[36] Argonne national laboratory, “EverBatt.” Accessed: June. 24, 2025. [Online]. Available: https://www.anl.gov/amd/everbatt.
[37] Ecoinvent, Carbon black production - ecoQuery [Online]. Available: https://ecoquery.ecoinvent.org/3.11/cutoff/dataset/7608/documentation. (Accessed 24 June 2025).
[38] A. Wu, R. Lindman, Current and future State of the European Li-ion battery recycling market [Online]. Available: www.ivl.se, 2022. (Accessed 7 July 2025).
[39] International energy agency, Price of selected battery materials and lithium-ion batteries [Online]. Available: https://www.iea.org/data-and-statistics/charts/price-of-selected-battery-materials-and-lithium-ion-batteries-2015-2024. (Accessed 28 July 2025).
[40] S&P. Global, Platts Black Mass Price Assessments, 2024.

[41] S. Orangi, N. Manjong, D.P. Clos, L. Usai, O.S. Burheim, A.H. Strømman, Historical and prospective lithium-ion battery cost trajectories from a bottom-up production modeling perspective, J. Energy Storage 76 (Jan. 2024) 109800, https://doi.org/10.1016/J.EST.2023.109800.

[42] Z. Chi, et al., Direct regeneration method of spent LiNi1/3Co1/3Mn1/3O2 cathode materials via surface lithium residues, Green Chem. 23 (22) (Nov. 2021) 9099–9108, https://doi.org/10.1039/D1GC03526F.

[43] S. Windisch-Kern, A. Holzer, C. Ponak, T. Hochsteiner, H. Raupenstrauch, Thermal analysis of lithium ion battery cathode materials for the development of a novel pyrometallurgical recycling approach, Carbon Resour. Convers. 4 (Jan. 2021) 184–189, https://doi.org/10.1016/J.CRCON.2021.04.005.

[44] V. Tiwari, G. Srivastava, Effect of thermal processing conditions on the structure and dielectric properties of PVDF films, J. Polym. Res. 21 (11) (Nov. 2014) 1–8, https://doi.org/10.1007/s10965-014-0587-0.

[45] H. Shin, R. Zhan, K.S. Dhindsa, L. Pan, T. Han, Electrochemical performance of recycled cathode active materials using froth flotation-based separation process, J. Electrochem. Soc. 167 (2) (Jan. 2020) 020504, https://doi.org/10.1149/1945-7111/AB6280.

[46] X. Li, J. Zhang, D. Song, J. Song, L. Zhang, Direct regeneration of recycled cathode material mixture from scrapped LiFePO4 batteries, J. Power Sources 345 (2017) 78–84, https://doi.org/10.1016/j.jpowsour.2017.01.118.

[47] V. Gupta, M. Appleberry, W. Li, Z. Chen, Direct recycling industrialization of Li-ion batteries: the pre-processing barricade, Next Energy 2 (Jan. 2024) 100091, https://doi.org/10.1016/J.NXENER.2023.100091.

[48] M. Wagner, D. Grießl, M. Hiller, A. Kwade, Characterization of Li-Ion cathode materials directly recycled via induction heating from production scraps, Electrochem. Soc. 172 (1) (2025), https://doi.org/10.1149/1945-7111/ada3a3.

[49] M. Ahuis, A. Aluzoun, M. Keppeler, S. Melzig, A. Kwade, Direct recycling of lithium-ion battery production scrap – Solvent-based recovery and reuse of anode and cathode coating materials, J. Power Sources 593 (Feb. 2024) 233995, https://doi.org/10.1016/J.JPOWSOUR.2023.233995.

[50] Y. Lai, et al., Recycling of spent LiFePO4 batteries by oxidizing roasting: kinetic analysis and thermal conversion mechanism, J. Environ. Chem. Eng. 11 (5) (Oct. 2023) 110799, https://doi.org/10.1016/J.JECE.2023.110799.

[51] H. Liu, et al., Thermal decomposition characteristics, products, and thermal transformation mechanisms of fluorine-containing organic components in lithium-ion batteries, J. Environ. Chem. Eng. 13 (6) (Dec. 2025) 120248, https://doi.org/10.1016/J.JECE.2025.120248.

[52] R. Dedryvère, M. Maccario, L. Croguennec, F. Le Cras, C. Delmas, D. Gonbeau, X-ray photoelectron spectroscopy investigations of carbon-coated Li xFePO4 materials, Chem. Mater. 20 (22) (Nov. 2008) 7164–7170, https://doi.org/10.1021/CM801995P/ASSET/IMAGES/LARGE/CM-2008-01995P_0007.JPEG.

[53] J. Nishanth, et al., Investigating the influence of PVDF binder crystallinity on the performance of LiFePO4 cathode in Li-ion batteries, Oxford Open Mater. Sci. 3 (1) (Jan. 2023), https://doi.org/10.1093/OXFMAT/ITAD019.

[54] M. Wang, et al., Challenges in recycling spent lithium-ion batteries: spotlight on polyvinylidene fluoride removal, Glob. Chall. 7 (3) (Mar. 2023) 2200237, https://doi.org/10.1002/GCH2.202200237.

[55] M. Abdollahifar, H. Cavers, S. Scheffler, A. Diener, M. Lippke, A. Kwade, Insights into influencing electrode calendering on the battery performance, Adv. Energy Mater. 13 (40) (Oct. 2023) 2300973, https://doi.org/10.1002/AENM.202300973.

[56] M. Bruno, C. Francia, S. Fiore, Selective leaching for the recycling of Lithium, Iron, and phosphorous from lithium-ion battery cathodes' production scraps, Batteries 10 (12) (Nov. 2024) 415, https://doi.org/10.3390/BATTERIES10120415, 2024, Vol. 10, Page 415.

[57] S. López Guzmán, C. Luengo, M. Reynaud, M. Galceran, M. Fehse, Direct recycling of cathode scrap: retain or remove residual binder and conductive carbon additives? J. Phys. Energy 7 (4) (Sep. 2025) 045024 https://doi.org/10.1088/2515-7655/AE09FB.

[58] E.C. Giles, A. Jarvis, A.T. Sargent, P.A. Anderson, P.K. Allan, P.R. Slater, Direct recycling of EV production scrap NMC532 cathode materials, RSC Sustain. 2 (10) (Oct. 2024) 3014–3021, https://doi.org/10.1039/D4SU00389F.

[59] L.E. Sita, et al., Direct recycling of LixNi0.5Mn0.3Co0.2O2 from production scrap and end-of-life batteries, using solid-state relithiation, Batter. Supercaps 8 (5) (May 2025) e202400536, https://doi.org/10.1002/BATT.202400536.

[60] N. Hayagan, et al., Direct recycling process using pressurized CO2 for Li-Ion battery positive electrode production scraps, ACS Sustain. Chem. Eng. 13 (1) (Jan. 2025) 105–118, https://doi.org/10.1021/ACSSUSCHEMENG.4C05591/ASSET/IMAGES/LARGE/SC4C05591_0008.JPEG.

[61] M. Wagner, D. Grießl, M. Hiller, A. Kwade, Induction heating as a pre-treatment for the recycling of Li-ion battery cathodes – technical feasibility, J. Clean. Prod. 428 (Nov. 2023) 139338, https://doi.org/10.1016/J.JCLEPRO.2023.139338.

[62] M.M. Gnutzmann, S. Raffenberg, M. Gutsch, M. Winter, M. Börner, J. Kasnatscheew, A dry-mechanical approach for scrap recycling of dry-processed lithium ion battery cathodes, Adv. Energy Mater. 15 (39) (Oct. 2025) e03459, https://doi.org/10.1002/AENM.202503459.

[63] A. Muguruza-Sánchez, et al., Direct recycling of graphite from spent batteries and production scraps for the development of a circular and sustainable economy, J. Power Sources Advan. 36 (Dec. 2025) 100191, https://doi.org/10.1016/J.POWERA.2025.100191.